Isotropic Properties of Some Multi-body Interaction Models: Two Quality Criteria for Markov Priors in Image Processing

Xavier Descombes, Eugene Pechersky

HAL Id: inria-00072910
https://inria.hal.science/inria-00072910

Submitted on 24 May 2006

INRIA

Isotropic properties of some multi-body interaction models: two quality criteria for Markov Priors in image processing

Xavier Descombes, Eugène Pechersky

N° 3752

Aout 1999

THÈME 3

Rapport de recherche

INRIA
SOPHIA ANTIPOLIS

Isotropic properties of some multi-body interaction models: two quality criteria for Markov Priors in image processing

Xavier Descombes, Eugène Pechersky

Thème 3 — Interaction homme-machine,
images, données, connaissances
Projet ARIANA

Abstract: Gibbs Fields are widely used in image processing for both segmentation and restoration. Defined on a discrete lattice representing the image they exhibit a non-isotropic behavior. Herein, we study and quantify this non-isotropy by computing the boundary tension as a function of the angle of a line separating the plane in two parts containing a different phase. From this study, we derive two quantitative criteria of the non isotropy of the model. We then compute the shape at zero temperature of a droplet of one phase within the other phase and study the non-isotropy of the shape for the different models. Finally, we show the artifacts due to this non-isotropic behavior for image segmentation and restoration.

Key-words: Gibbs Fields, Isotropy, Quality criteria, Image Segmentation and Restoration

Propriétés d'isotropie de certains modèles à interactions multi-corps : deux critères de qualité pour les modèles a priori de type markovien en traitement d'image

Résumé : Les champs de Gibbs sont très utilisés en traitement d'image à la fois pour la segmentation et la restauration. Définis sur la trâme discrète sous-jacente à l'image, ils présentent un comportement non isotrope. Dans ce rapport, nous étudions et quantifions cette non-isotropie, pour des modèles avec des interactions 3x3, en calculant la tension de bord en fonction de l'angle d'une droite séparant le plan en deux parties contenant une phase différente. De cette étude, nous dérivons deux critères quantitatifs d'anisotropie des modèles. Nous calculons ensuite la forme d'une goutte d'une phase immergée dans une autre phase à la température nulle pour les différents modèles, et étudions la non isotropie des formes obtenues. Pour finir, les artéfacts induits par cette non-isotropie sont mis en évidence sur des exemples de segmentation et de restauration d'image.

Mots-clés : Champs de Gibbs, Isotropie, Critères de qualité, Segmentation et Restauration d'Image

Contents

1 Introduction

Applications of the Gibbs field theory in image restoration and segmentation can be divided into three parts. The first part consists in choosing a model. The second one is the parameter estimation problem. The last one corresponds to the optimization of the chosen model. The chosen model may induce some undesired properties in the result. One of such properties which is the subject of our investigation hereafter is the non-isotropic behavior of models. It seems to be obvious that the result of an image treatment must not depend on the rotation of the camera with respect to the vertical axis, if the image was obtained by a photography from above. However the digital image is, in most cases, a configuration on the square lattice $\mathbb{Z}^2$ which has rather poor isotropic properties. Therefore finding a Gibbs model which is isotropic as much as possible is quite an actual problem.

Herein, we restrict ourselves to the study of the isotropic properties of a class of models with respect to big objects. One can say we study the isotropic properties of two dimensional objects. Further work will be devoted to small objects or to one dimensional objects, such as lines.

Any Gibbs field is defined by its potential functions. In Gibbs field applications to image processing, a Gibbs field is composed of two terms. The first term describes a Gibbs model used in the problem. With the statistical point of view, the Gibbs model defines a prior distribution within a Bayesian. The second type of potential functions, corresponding to the likelihood in the Bayesian approach, is a Gibbs model introducing data in the Gibbs field (for examples, see [5, 8]). The prior model is introduced within a Bayesian framework to add some spatial homogeneity constraints on the solution. However, some artifacts can also be introduced. The study of such artifacts motivates work presented hereafter.

Our goal is to study the Gibbs model giving the prior distribution. All considered models are defined on $\mathbb{Z}^2$ with the two-point spin space $X = \{0, 1\}$. We first study the behavior of the models for configurations consisting of two half-planes. Let $\underline{n} = (n_1, n_2)$ be a unit vector in $\mathbb{R}^2$. Consider the configuration $x(t)$ on $\mathbb{Z}^2$ such that:

$$x(t) = \begin{cases} 0, & \text{if } t_1 n_1 + t_2 n_2 > 0, \\ 1, & \text{if } t_1 n_1 + t_2 n_2 \le 0. \end{cases}$$

We want to know the boundary tension of the line $r_1 n_1 + r_2 n_2 = 0$, $(r_1, r_2) \in \mathbb{R}^2$. The boundary tension is a specific energy $\tau_{\underline{n}}$ of interactions over this line. The isotropy (in the sense we study hereafter) means that the specific energy does not depend on the vector $\underline{n}$. Of course, the models we study are not isotropic. We conjecture that there is no model with finite range interactions on $\mathbb{Z}^2$ having this property. We propose to evaluate the non-isotropy of models with finite range interactions. More precisely, we study the models having the clique sets bounded in a 3×3 site square. This class includes a rather wide set

of models. In particular, the Ising model belongs to this class.

We find the boundary tension τ_γ as a function of $\gamma = \frac{n_1}{n_2}$ for the pointed models. We calculate minimal values of τ_γ and the corresponding values of γ. A special interest is the number of values γ giving the minimal value τ_γ. We show that, depending on the model, this number can take the values 4,8,12 and 16. Two criteria are derived to quantify the non isotropy of the studied models.

Then, we describe the isotropy properties of models by studying droplets of one phase inside another, for example the droplet of the phase combined by 0's in the phase combined by 1's. We use Wulff construction to obtain the shapes of the droplets at zero temperature (see [7, 10]). Our result is not a theorem because we do not use the rigorous definition of the surface tension. Therefore we call the function τ_γ the boundary tension instead of the surface tension which is commonly used. We conjecture that, in fact, τ_γ is the surface tension at zero temperature. We shall study this problem in a near future. At the pointed setting, we have found polygons giving shapes of the droplets.

Doing as mentioned above, we have found three basic shapes of the droplets for the different studied models. There are also a set of models for which the shapes are "mixtures" of the basic shapes. There are only two parameters (g, h) for the models which control the droplet shapes.

Finally, we perform some experiments on image segmentation and image restoration to show the artifacts due to this anisotropic effect. We compare the usual Ising model with a 8-neighbors interaction Ising model and the Chien-model defined in [1, 6, 9].

2   3x3 models

2.1   Assumptions

To describe the studied models, we introduce a set $\mathcal{V}$ of cliques and for every clique $V \in \mathcal{V}, \quad V \subset \mathbb{Z}^2$, a potential function:

$$\Phi_V : \ X^V \to \mathbb{R}. \tag{1}$$

We recall that $X = \{0, 1\}$. Because we consider the translation invariant models, we can only describe the cliques containing the site $0 \in \mathbb{Z}^2$. Let $\mathcal{V}_0$ be this set. In the 3x3 models, every clique $V \in \mathcal{V}_0$ is a subset of the set:

$$W = \{t = (t_1, t_2) \in \mathbb{Z}^2 : \ |t_i| \leq 1, i = 1, 2\}. \tag{2}$$

We do not loose any generality if we take the set $\mathcal{V}_0$ containing only the clique W. Then we only have to define a potential function Φ which assigns an energy value to configurations

x_W on W, $x_W \in X^W$. Since the potential function Φ is invariant with respect to the translations of $\mathbb{Z}^2$, we consider Φ as a function of 9 variables.

Now we give the main assumptions on Φ. We call a tile a table of nine numbers:

$$\overline{r} = \begin{pmatrix} r_{11} & r_{12} & r_{13} \\ r_{21} & r_{22} & r_{23} \\ r_{31} & r_{32} & r_{33} \end{pmatrix}, \tag{3}$$

where $r_{ij} \in \{0, 1\}$. We consider the function Φ as a function of tiles. Φ can generally take 2^9 values. However, we require that Φ is invariant with the respect natural symmetries of tiles. Let $\overline{r}$ be a tile. All rotations of $\overline{r}$ and reflections with respect to horizontal and vertical axes and with respect to the both diagonals compose a group $\widehat{G}$ of tile changes. Besides we add to $\widehat{G}$ flips of $\overline{r}$ taking every r_{ij} to $1 + r_{ij} \pmod 2$. Let G be the complete group of the described actions on $\overline{r}$.

We assume that the following four conditions on the function Φ are satisfied:
Condition $\Phi 0$

$$\Phi(\overline{r}) = \Phi(g(\overline{r})),$$

where $g \in G$ and $\overline{r}$ is a tile.

This condition reduces the 2^9 possible values of Φ to 51.

Let $\overline{v}_0 = \begin{pmatrix} 0 & 0 & 0 \\ 0 & 0 & 0 \\ 0 & 0 & 0 \end{pmatrix}$ and $\overline{v}_1 = \begin{pmatrix} 1 & 1 & 1 \\ 1 & 1 & 1 \\ 1 & 1 & 1 \end{pmatrix}$. We normalize the values of Φ by assuming that:
Condition $\Phi 1$

$$\Phi(\overline{v}_0) = \Phi(\overline{v}_1) = 0.$$

Consider the following tiles:

$$\overline{u}_0 = \begin{pmatrix} 0 & 0 & 0 \\ 1 & 1 & 1 \\ 1 & 1 & 1 \end{pmatrix}$$

$$\overline{u}_1^1 = \begin{pmatrix} 0 & 1 & 1 \\ 1 & 1 & 1 \\ 1 & 1 & 1 \end{pmatrix} \quad \overline{u}_1^2 = \begin{pmatrix} 0 & 0 & 1 \\ 0 & 1 & 1 \\ 1 & 1 & 1 \end{pmatrix}$$

$$\overline{u}_2^1 = \begin{pmatrix} 0 & 0 & 1 \\ 1 & 1 & 1 \\ 1 & 1 & 1 \end{pmatrix} \quad \overline{u}_2^2 = \begin{pmatrix} 0 & 0 & 0 \\ 0 & 1 & 1 \\ 1 & 1 & 1 \end{pmatrix}$$

The next assumptions restrict the values of Φ on the above tiles:
   Condition $\Phi 2$

$$\Phi(\overline{u}_0) > 0,$$
$$\Phi(\overline{u}_1^1) + \Phi(\overline{u}_1^2) > 0,$$
$$\Phi(\overline{u}_1^1) + \Phi(\overline{u}_2^1) + \Phi(\overline{u}_2^2) > 0.$$

Let $\Phi(\overline{u}_0) = e$. Let h and g be positive numbers such that:

$$\Phi(\overline{u}_1^1) + \Phi(\overline{u}_1^2) = he,$$
$$\Phi(\overline{u}_1^1) + \Phi(\overline{u}_2^1) + \Phi(\overline{u}_2^2) = ge.$$

The next condition ensure that our models are of ferromagnetic type. Consider a table $\overline{\overline{s}} = (s_{ij})_{1 \le i,j \le 5}$, where $s_{ij} \in \{0,1\}$. Let $\mathcal{P}_{\overline{\overline{s}}} = \{\overline{r}\}$ be the set of all tiles $\overline{r}$ which can be extracted from $\overline{\overline{s}}$.

   Condition $\Phi 3$
   If $\overline{\overline{s}}$ is not the constant 0 or 1 then:

$$\sum_{\overline{r} \in \mathcal{P}_{\overline{\overline{s}}}} \Phi(\overline{r}) > 0.$$

It is obvious from conditions $\Phi 0$–$\Phi 3$ that the configurations $v^0(t) \equiv 0$ and $v^1(t) \equiv 1$ are periodical ground states and there are no other ones. Of course, there are infinite many non-periodical ground states whose types depend on the values of h and g. It is also easy to see that the Peierls conditions are satisfied [4]. Therefore, there exists a critical temperature separating the case of the unique Gibbs state and the case of two (at least) Gibbs states.

2.2   Examples

First we discuss an example of models which only have pair interactions. The well-known Ising model is a particular case of the models considered in this section.

If $x \in X^{\mathbb{Z}^2}$ is a configuration then x_W is the restriction of x on W (see eqn. (2)). We denote $W_t = W + t$ where $t \in \mathbb{Z}^2$. The sets W and W_t are called plaquettes. Let:

$$R = \{1, \sqrt{2}, 2, \sqrt{5}, 2\sqrt{2}\} \tag{4}$$
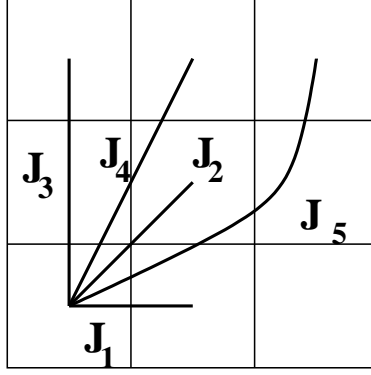
Figure 1: Pairwise interactions in the 3×3 site square

be the set of distances between pairs of sites (see figure 1).

We consider models with the formal Hamiltonian

$$\widehat{H}(\mathbf{x}) = -\sum_{i=1}^{5} J_i \sum_{|t-s|=\rho_i} [2x(t) - 1][2x(s) - 1], \tag{5}$$

where $\rho_i \in R$ such that ρ_i is equal to the i-th number in (4), for example, $\rho_4 = \sqrt{5}$. Next we represent eqn. (5) as a double sum, the inner is over pairs of sites in a plaquette and the outer is over all plaquettes:

$$\widehat{H}(\mathbf{x}) = -\sum_{u \in \mathbb{Z}^2} \sum_{i=1}^{5} \frac{J_i}{n_i} \sum_{\substack{t,\, s\, \in\, W_u \\ |t-s|\, =\, \rho_i}} [2x(t) - 1][2x(s) - 1], \tag{6}$$

where n_i are as follows: $n_1 = 6$, $n_2 = 4$, $n_3 = 3$, $n_4 = 2$, $n_5 = 1$. The value n_i is the number of plaquettes which contain a pair of sites for which the distance between the sites is equal to ρ_i. To meet the condition $\Phi 1$, we change the Hamiltonian described in eqn. (6) in a way which does not change the model. Namely, we introduce the potential function Φ:

$$\Phi(\overline{r}) = -\sum_{i=1}^{5} \left[\frac{J_i}{n_i} \sum_{|(k,l)-(m,n)|=\rho_i} [2r_{k,l} - 1][2r_{m,n} - 1] - J_i a_i \right], \tag{7}$$

where $a_i = \begin{cases} 2, & \text{if } i \neq 4 \\ 4, & \text{if } i = 4 \end{cases}$, and $\overline{r}$ is a tile (see eqn. (3)). We added the constant $\sum_{i=1}^{5} a_i J_i$ to the energy of every tile in eqn. (6) such that the energy of the tiles $\overline{v}_0$ and $\overline{v}_1$ is equal

to 0, which gives the condition $\Phi 1$. The condition $\Phi 0$ is obviously satisfied.

Up to now, we did not impose any condition on the constants $J_1, \ldots, J_5$. Next, we consider the condition $\Phi 2$. We have:

$$e = \Phi(\overline{u}_0) = J_1 + 2J_2 + 2J_3 + 6J_4 + 4J_5 \tag{8}$$

The first inequality of condition $\Phi 2$ requires the positivity of the above sum. The following equations give the energy of all other tiles involved in condition $\Phi 2$:

$$\Phi(\overline{u}_1^1) = \frac{2}{3}J_1 + \frac{1}{2}J_2 + \frac{4}{3}J_3 + 2J_4 + 2J_5$$

$$\Phi(\overline{u}_1^2) = \frac{4}{3}J_1 + \frac{3}{2}J_2 + \frac{8}{3}J_3 + 6J_4 + 2J_5$$

$$\Phi(\overline{u}_2^1) = J_1 + \frac{3}{2}J_2 + 2J_3 + 4J_4 + 2J_5$$

$$\Phi(\overline{u}_2^2) = \frac{4}{3}J_1 + 2J_2 + \frac{8}{3}J_3 + 6J_4 + 4J_5.$$

The last two inequalities in condition $\Phi 2$ give the following relations:

$$\begin{aligned} he &= 2J_1 + 2J_2 + 4J_3 + 8J_4 + 4J_5 > 0, \\ ge &= 3J_1 + 4J_2 + 6J_3 + 12J_4 + 8J_5 > 0. \end{aligned} \tag{9}$$

It is clear that if all the constants $J_1, \ldots, J_5$ are positive then condition $\Phi 3$ holds. We do not loose any generality if we put

$$2e = 1 \tag{10}$$

Further we shall assume that eqn. (10) is fulfilled. The new Hamiltonian is then:

$$H(x) = \sum_{u \in \mathbb{Z}^2} \Phi(x_{W_u}). \tag{11}$$

Remark that the specifications defined by both Hamiltonians in eqn. (6) and (11) are the same.

We consider some particular cases of the models described by eqn. (7):

Model 1: Let $J_2 = J_3 = J_4 = J_5 = 0$. Then we have the Ising model with $e = \frac{1}{2}$, $h = 2$, $g = 3$.

Model 2: In the next example, we assume that $J_3 = J_4 = J_5 = 0$. For this case (called the 8-connected Ising model in the image processing community), recalling that $e = \frac{1}{2}$, we have:

$$J_1 + 2J_2 = \frac{1}{2},$$
$$g = 2 + 2J_1, \tag{12}$$
$$h = 1 + 2J_1.$$

Hence $J_1 > -\frac{1}{2}$ to satisfy $\Phi 2$. If $J_1 = \frac{1}{2}$ then $J_2 = 0$ and we have the previous case. Remark also that for $J_1 < 0$, the configuration:

$$x(t) = \begin{cases} 1, & \text{if } |t_1| + |t_2| = 2l, \\ 0, & \text{if } |t_1| + |t_2| = 2l + 1 \end{cases} \tag{13}$$

has a negative energy. Namely:

$$\sum_{P:\, 0 \in P} \Phi(x_P) = 36 J_1,$$

where P is a plaquette. Hence $\Phi 3$ is not satisfied. The direct calculations show that for $J_1 > \frac{1}{2}$ (in this case $J_2 < 0$), the energy of every tile, except v^0 and v^1, is positive. It means that $\Phi 3$ holds.

3   The boundary tension

3.1   Computation of the boundary tension

The first result concerns the boundary tension. Herein, we give the exact definition of this notion. Let $\underline{n} = (n_1, n_2)$ be a unit vector, and $x^\gamma \in X^{\mathbb{Z}^2}$ the configuration on $\mathbb{Z}^2$ such that:

$$x^\gamma = \begin{cases} 1, & \text{if } n_1 t_1 + n_2 t_2 > 0, \\ 0, & \text{otherwise} \end{cases}$$

where $\gamma = \frac{n_2}{n_1}$. We evaluate the energy of interactions over the line $L_\gamma = \{(r_1, r_2) : n_1 r_1 + n_2 r_2 = 0\}$.

Let $W_t = W + t$, where $t \in \mathbb{Z}^2$ (see eqn. (2)). Let also:

$$\overline{W} = \{r = (r_1, r_2) \in \mathbb{R}^2 : |r_i| \le 1, i = 1, 2\}$$

and

$$\overline{W}_t = \overline{W} + t.$$

Finally, let for $z > 0$:

$$U_\gamma(z) = \{t = (t_1, t_2) \in \mathbb{Z}^2 : \overline{W}_t \cap L_\gamma \neq \emptyset, |t_1| \leq z\} \tag{14}$$

Let x be a configuration, then the energy of the projection $x^\gamma_{U_\gamma(z)}$ is:

$$H_{U_\gamma(z)}(x^\gamma) = \sum_{t \in U_\gamma(z)} \Phi(x^\gamma_{W_t})$$

The boundary tension of the slope γ is:

$$\widetilde{\tau}_\gamma = \lim_{z \to \infty} \frac{H_{U_\gamma(z)}(x^\gamma)}{2z\sqrt{1+\gamma^2}} \tag{15}$$

Theorem 1 *The boundary tension has the following form:*

$$\tau_\gamma = \begin{cases} \frac{2\gamma[g-2]+2}{\sqrt{1+\gamma^2}} e, & \text{if } \gamma \leq \frac{1}{2}, \\ \frac{2[\gamma(2h-g)+(g-h)]}{\sqrt{1+\gamma^2}} e, & \text{if } \frac{1}{2} \leq \gamma \leq 1. \end{cases} \tag{16}$$

Proof. Let $t = (t_1, t_2), u = (t_1, u_2) \in \mathbb{Z}^2$ be such that:

   1) $\overline{W}_t \cap L_\gamma \neq \emptyset$,
2) $\overline{W}_{(t_1, t_2-1)} \cap L_\gamma = \emptyset$,
3) $\overline{W}_u \cap L_\gamma \neq \emptyset$,
4) $\overline{W}_{(t_1, u_2+1)} \cap L_\gamma = \emptyset$.

We shall study separately the cases $\gamma \leq \frac{1}{2}$ and $\gamma \geq \frac{1}{2}$. In the first case, the sequence of the tiles

$$x^\gamma_{W_{(t_1,t_2)}}, x^\gamma_{W_{(t_1,t_2+1)}}, \ldots, x^\gamma_{W_{(t_1,u_2)}} \tag{17}$$

is either

$$\begin{pmatrix} 0 & 0 & 0 \\ 1 & 1 & 1 \\ 1 & 1 & 1 \end{pmatrix} \begin{pmatrix} 0 & 0 & 0 \\ 0 & 0 & 0 \\ 1 & 1 & 1 \end{pmatrix} \tag{18}$$

or

$$\begin{pmatrix} 1 & 0 & 0 \\ 1 & 1 & 1 \\ 1 & 1 & 1 \end{pmatrix} \begin{pmatrix} 0 & 0 & 0 \\ 1 & 0 & 0 \\ 1 & 1 & 1 \end{pmatrix} \begin{pmatrix} 0 & 0 & 0 \\ 0 & 0 & 0 \\ 1 & 0 & 0 \end{pmatrix} \tag{19}$$

or

$$\begin{pmatrix} 1 & 1 & 0 \\ 1 & 1 & 1 \\ 1 & 1 & 1 \end{pmatrix} \begin{pmatrix} 0 & 0 & 0 \\ 1 & 1 & 0 \\ 1 & 1 & 1 \end{pmatrix} \begin{pmatrix} 0 & 0 & 0 \\ 0 & 0 & 0 \\ 1 & 1 & 0 \end{pmatrix}. \tag{20}$$

The energy sum of the first sequence is $2e$ and the sum of the two last sequences is ge (see condition $\Phi 2$). Remark that the two last sequences appear simultaneously. Therefore their contribution to the energy is equal to $2ge$ when they appear. We calculate the frequency $\rho = \rho(\gamma)$ of that appearance as a function of γ. Since $\gamma \leq \frac{1}{2}$, there exists $k \geq 2$ such that $\frac{1}{k+1} \leq \gamma < \frac{1}{k}$. Let the pairs $t = (t_1, t_2)$, $u = (t_1, u_2)$ and $t' = (t'_1, t'_2)$, $u' = (t'_1, u'_2)$ satisfy conditions 1)—4) above and $t'_1 = t_1 + 1$ then for considered case $t_2 - t'_2 \leq 1$. If $t_2 - t'_2 = 1$ then we have a jump down at which the two last sequences of (18) appear. Let N_z be a number of the jumps down in the set $U_\gamma(z)$ (see eqn. (14)). Then $\lim_{z \to \infty} \frac{N_z}{2z} \to \gamma$. Therefore, the total number M_z of appearances of the two mentioned sequences of the plaquettes are estimated as follows:

$$4z\gamma(1 - \varepsilon) \leq M_z \leq 4z\gamma(1 + \varepsilon)$$

for any ε when z is large enough. Every pair of the sequences gives the energy contribution equal to ge. The number of the first sequence of (18) is $2z - M_z$. Therefore the total energy of the set $U_\gamma(z)$ is estimated as:

$$2z[2\gamma ge + (1 - 2\gamma)e](1 - \varepsilon) \leq H_{U_\gamma(z)}(x^\gamma) \leq 2z[2\gamma ge + (1 - 2\gamma)e](1 + \varepsilon). \tag{21}$$

Hence, the boundary tension for $0 \leq \gamma \leq \frac{1}{2}$ is:

$$\tau_\gamma = \frac{2\gamma[g - 2] + 2}{\sqrt{1 + \gamma^2}} e. \tag{22}$$

Next, we study the case $\frac{1}{2} \leq \gamma \leq 1$. Then the sequence: (17) is either

$$\begin{pmatrix} 1 & 0 & 0 \\ 1 & 1 & 1 \\ 1 & 1 & 1 \end{pmatrix} \begin{pmatrix} 0 & 0 & 0 \\ 1 & 0 & 0 \\ 1 & 1 & 1 \end{pmatrix} \begin{pmatrix} 0 & 0 & 0 \\ 0 & 0 & 0 \\ 1 & 0 & 0 \end{pmatrix}$$

or

$$\begin{pmatrix} 1 & 1 & 0 \\ 1 & 1 & 1 \\ 1 & 1 & 1 \end{pmatrix} \begin{pmatrix} 0 & 0 & 0 \\ 1 & 1 & 0 \\ 1 & 1 & 1 \end{pmatrix} \begin{pmatrix} 0 & 0 & 0 \\ 0 & 0 & 0 \\ 1 & 1 & 0 \end{pmatrix}$$

or

$$\begin{pmatrix} 1 & 1 & 0 \\ 1 & 1 & 1 \\ 1 & 1 & 1 \end{pmatrix} \begin{pmatrix} 1 & 0 & 0 \\ 1 & 1 & 0 \\ 1 & 1 & 1 \end{pmatrix} \begin{pmatrix} 0 & 0 & 0 \\ 1 & 0 & 0 \\ 1 & 1 & 0 \end{pmatrix} \begin{pmatrix} 0 & 0 & 0 \\ 0 & 0 & 0 \\ 1 & 0 & 0 \end{pmatrix}$$

The energy of the last sequence is $2h$ (see condition $\Phi 2$). Producing considerations close to those done for the case $\gamma \le \frac{1}{2}$, we obtain that the frequency of the last sequence is $2\gamma - 1$. The analogue of the inequality (21) is:

$$2z[2(1-\gamma)ge + (2\gamma-1)2he](1-\varepsilon) \le H_{U_\gamma(z)}(x^\gamma) \le 2z[2(1-\gamma)ge + (2\gamma-1)2he](1+\varepsilon) \tag{23}$$

Applying definition (15), we obtain:

$$\tau_\gamma = \frac{2[\gamma(2h-g) + (g-h)]}{\sqrt{1+\gamma^2}}e \quad \square \tag{24}$$

3.2   Study of the boundary tension minima

This subsection is devoted to the study of the minima of the boundary tension τ_γ. Let:

$$\Delta_1^1 = \left\{ (h, g) : 0 < h < \sqrt{\frac{2}{5}}g, \, 0 < g \le \sqrt{5} \right\},$$

$$\Delta_1^2 = \left\{ (h, g) : 0 < h < \sqrt{2}, \, g > \sqrt{5} \right\},$$

$$\Delta_1 = \Delta_1^1 \cup \Delta_1^2,$$

$$\Delta_2 = \left\{ (h, g) : h > \sqrt{\frac{2}{5}}g, \, 0 < g \le \sqrt{5} \right\},$$

$$\Delta_3 = \left\{ (h, g) : h > \sqrt{2}, \, g > \sqrt{5} \right\}.$$

Δ_1, Δ_2 and Δ_3 are open sets. Depending on the values of h and g, there are three values of γ where τ_γ attains its minimum. More precisely, let $\Gamma(h, g) \subset [0, 1]$ be the set of γ where this minimum is attained then we have:

Corollary 2

$$\Gamma_1 = \Gamma(h, g) = \{1\}, \qquad\qquad\qquad if\ (h, g) \in \Delta_1,$$

$$\Gamma_2 = \Gamma(h, g) = \{\frac{1}{2}\}, \qquad\qquad\qquad if\ (h, g) \in \Delta_2,$$

$$\Gamma_3 = \Gamma(h, g) = \{0\}, \qquad\qquad\qquad if\ (h, g) \in \Delta_3.$$

Moreover, on the common boundary of the sets Δ_i and Δ_j, we have:

$$\Gamma_{ij} = \Gamma(h, g) = \Gamma_i \cup \Gamma_j,$$

where $(h, g) \in \partial\Delta_i \cap \partial\Delta_j$.

Finally at the point $\left(\sqrt{5}, \sqrt{2}\right)$ which is $\partial\Delta_1 \cap \partial\Delta_2 \cap \partial\Delta_3$, we get:

$$\Gamma\left(\sqrt{2}, \sqrt{5}\right) = \Gamma_1 \cup \Gamma_2 \cup \Gamma_3 = \left\{0, \frac{1}{2}, 1\right\}.$$

Proof. First we study the case $\gamma \in \left[0, \frac{1}{2}\right]$. Taking $e = \frac{1}{2}$ we have the following derivatives:

$$\tau'_\gamma = \frac{g - 2 - \gamma}{(1 + \gamma^2)^{\frac{3}{2}}}$$

and

$$\tau''_\gamma = \frac{2\gamma^2 - 3\gamma(g - 2) - 1}{(1 + \gamma^2)^{\frac{5}{2}}}.$$

For small γ the second derivative is negative. It means that τ_γ is concave in the region of small γ. Let $\gamma_0 \in \left(0, \frac{1}{2}\right)$ be a point such that on the interval $(0, \gamma_0)$ the function τ_γ is concave. Remark that at the point:

$$\gamma_1 = g - 2,$$

where the first derivative is equal to 0, the second derivative takes a negative value:

$$\frac{-(g - 2)^2 - 1}{(1 + \gamma_1^2)^{\frac{5}{2}}}.$$

Therefore γ_1 is the point of a local maximum of τ_γ. There is no other value of γ in the interval $\left[0, \frac{1}{2}\right]$ such that $\tau'_\gamma = 0$. Hence there are no local minima of τ_γ for $\gamma \geq \gamma_0$ where τ_γ is convex. It proves that, on the interval $\left[0, \frac{1}{2}\right]$, the minima values can be attained on the ends of this interval.

Next we study τ_γ on $\left[\frac{1}{2}, 1\right]$. We have:

$$\tau_\gamma' = \frac{\gamma(h-g) + 2h - g}{(1+\gamma^2)^{\frac{3}{2}}}$$

and

$$\tau_\gamma'' = \frac{-2\gamma^2(h-g) - 3\gamma(2h-g) - h - g}{(1+\gamma^2)^{\frac{5}{2}}}$$

As in previous case, we have only the point:

$$\gamma_2 = \frac{g - 2h}{h - g},$$

where the function τ_γ has a local minimum. The second derivative at this point is:

$$\frac{(g-2h)^2 + (h-g)^2}{h-g} \frac{1}{(1+\gamma_2^2)^{\frac{5}{2}}}. \tag{25}$$

Hence, its sign depends on the relation between h and g. Eqn. (25) takes the positive value at a negative γ_2. Therefore, we obtain that minimal values of τ_γ are attained on the ends of the interval $\left[\frac{1}{2}, 1\right]$. The result follows now from the expression (16). $\square$

We have shown the non isotropic behavior of the studied models. The different curves plotted on figure 2 show the boundary tension for different models. Figure 2.a corresponds to an Ising model for which $e = \frac{1}{2}$, $(h, g) = (2, 3)$. We have a single minimum for the boundary tension. Using an Ising model with 8 neighbors, we can set the parameters in order to have two minima for the boundary tension. Figure 2.b shows such an example for $e = \frac{1}{2}$, $(h, g) = (\sqrt{2}, 1 + \sqrt{2})$. Finally, the least non isotropic models correspond to $e = \frac{1}{2}$, $(h, g) = (\sqrt{2}, \sqrt{5})$, as shown on figure 2.c. Such an example is given by the Chien-model described in [9].

3.3 A first criterion to quantify the non isotropy

In order to compare the different models and the to assess their quality with respect to isotropy, we propose to define a criterion based on the boundary tension. This criterion reflects the average fluctuations with respect to minimal boundary tension. It is defined as follows:

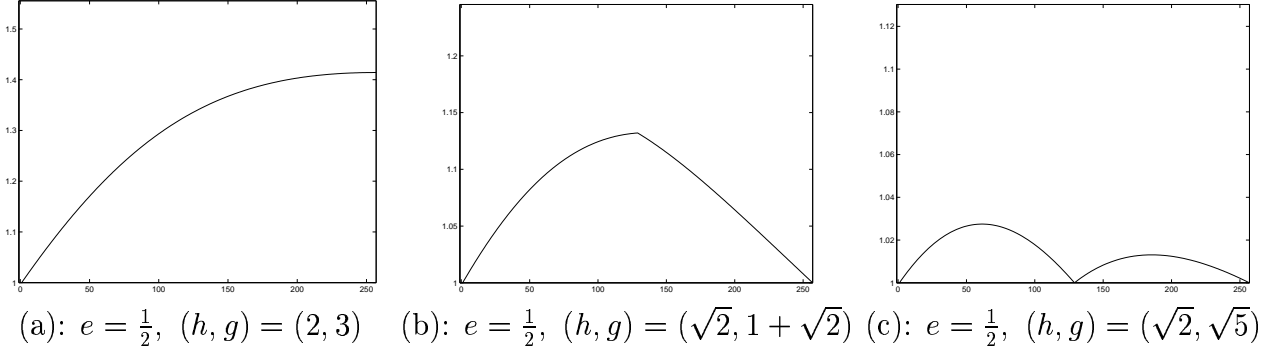$$ANIS_1 = \frac{\int_0^1 \tau_\gamma d\gamma}{\min_{[0,1]} \tau_\gamma}. \tag{26}$$

(a): $e = \frac{1}{2}$, $(h, g) = (2, 3)$ (b): $e = \frac{1}{2}$, $(h, g) = (\sqrt{2}, 1 + \sqrt{2})$ (c): $e = \frac{1}{2}$, $(h, g) = (\sqrt{2}, \sqrt{5})$

Figure 2: Boundary tension for model 1 (a), model 2 (b) and the Chien-model (c) (X-axis: $256 * \gamma$, Y-axis: τ_γ)

For an isotropic model, we have $ANIS_1 = 1$.

Recalling that:

$$I_1 = \int_0^{\frac{1}{2}} \frac{d\gamma}{\sqrt{1 + \gamma^2}} = \log 2 - \log\left(-1 + \sqrt{5}\right), \tag{27}$$

$$I_2 = \int_{\frac{1}{2}}^1 \frac{d\gamma}{\sqrt{1 + \gamma^2}} = \log\left(\sqrt{2} - 1\right) + \log 2 - \log\left(-1 + \sqrt{5}\right), \tag{28}$$

$$I_3 = \int_0^{\frac{1}{2}} \frac{\gamma d\gamma}{\sqrt{1 + \gamma^2}} = \frac{1}{2}\sqrt{5} - 1, \tag{29}$$

$$I_4 = \int_{\frac{1}{2}}^1 \frac{\gamma d\gamma}{\sqrt{1 + \gamma^2}} = \sqrt{2} - \frac{1}{2}\sqrt{5}, \tag{30}$$

and therefore, for the studied models:

$$I(g, h) = \int_0^1 \tau_\gamma d\gamma = (g - 2)I_1 + I_3 + (2h - g)I_2 + (g - h)I_4, \tag{31}$$

we obtain the following expressions:

$$ANIS_1(g, h) = I(g, h) \quad \text{if } g \geq \sqrt{5} \text{ and } h \geq \sqrt{2}, \tag{32}$$

$$ANIS_1(g, h) = \frac{\sqrt{2}I(g,h)}{h} \quad \text{if } \sqrt{2}g \geq \sqrt{5}h \text{ and } h \leq \sqrt{2}, \tag{33}$$

$$ANIS_1(g, h) = \frac{\sqrt{5}I(g,h)}{g} \quad \text{if } \sqrt{2}g \leq \sqrt{5}h \text{ and } g \leq \sqrt{5}. \tag{34}$$

Figure 3 shows the values of $ANIS_1(g, h)$ in the (g, h) plane. The minimum is obtained for $(g, h) = (\sqrt{2}, \sqrt{5})$. This corresponding value represents a minimal bound for 3×3 models on a square lattice.
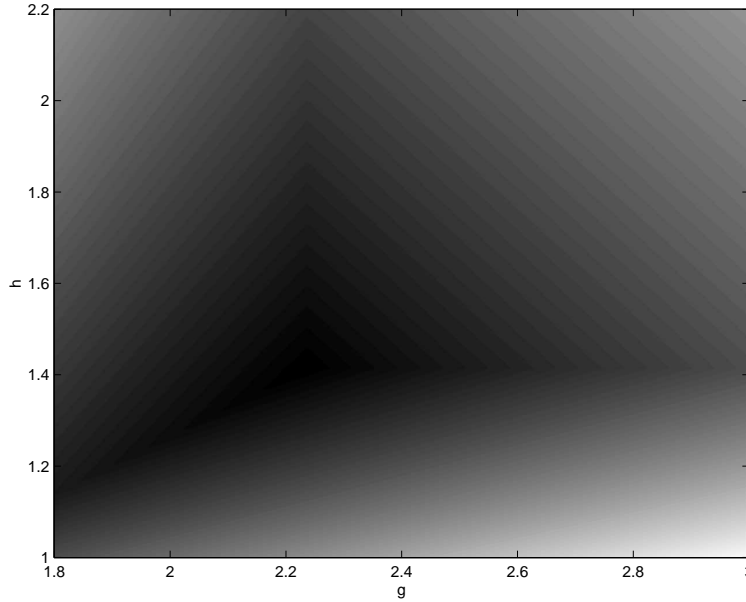

Figure 3: The criterion $ANIS_1$ in the (g, h) plane (dark (resp. light) values represent low (resp. high) values) of the criterion

3.4 A second criterion to quantify the non isotropy

The first criterion can be interpreted as an average non-isotropy ratio. We now quantify the maximum of the ratio. Therefore, we define a second criterion as follows:

$$ANIS_2(g, h) = \frac{\max_{[0,1]} \tau_\gamma(g, h)}{\min_{[0,1]} \tau_\gamma(g, h)}. \tag{35}$$

We obtain an isotropic model if and only if $ANIS_2(g, h) = 1$. We study the values where the derivative is equal to 0 and their position with respect to 0, $\frac{1}{2}$ and 1. The minimum and maximum values of τ_γ for $\gamma \in [0, \frac{1}{2}]$ and $\gamma \in [\frac{1}{2}, 1]$, depending on (g, h), are respectively given in Tables 1 and 2. We then have:

$$ANIS_2(g, h) = \frac{\max\left(\max_{[0,\frac{1}{2}]} \tau_\gamma(g, h), \max_{[\frac{1}{2},1]} \tau_\gamma(g, h)\right)}{\min\left(\min_{[0,\frac{1}{2}]} \tau_\gamma(g, h), \min_{[\frac{1}{2},1]} \tau_\gamma(g, h)\right)}. \tag{36}$$

| g	$g \leq 2$	$2 \leq g \leq \sqrt{5}$	$\sqrt{5} \leq g \leq \frac{5}{2}$	$g \geq \frac{5}{2}$
min	$\frac{2ge}{\sqrt{5}}$	$\frac{2ge}{\sqrt{5}}$	$2e$	$2e$
max	$2e$	$2e\sqrt{(g-2)^2+1}$	$2e\sqrt{(g-2)^2+1}$	$\frac{2ge}{\sqrt{5}}$

Table 1: Minimum and maximum values of τ_γ for $\gamma \in [0, \frac{1}{2}]$ in the (g, h) plane

h	$h \leq \frac{3}{5}g$	$\frac{3}{5}g \leq h \leq \frac{\sqrt{2}}{\sqrt{5}}g$	$\frac{\sqrt{2}}{\sqrt{5}}g \leq h \leq \frac{2}{3}g$	$h \geq \frac{2}{3}g$
min	$\frac{2he}{\sqrt{2}}$	$\frac{2he}{\sqrt{2}}$	$\frac{2ge}{\sqrt{5}}$	$\frac{2ge}{\sqrt{5}}$
max	$\frac{2ge}{\sqrt{5}}$	$2e\sqrt{(2h-g)^2+(g-h)^2}$	$2e\sqrt{(2h-g)^2+(g-h)^2}$	$\frac{2he}{\sqrt{2}}$

Table 2: Minimum and maximum values of τ_γ for $\gamma \in [\frac{1}{2}, 1]$ in the (g, h) plane

Figure 4 shows the values of $ANIS_2(g, h)$ in the (g, h) plane. Once again, the minimum is obtained for $(g, h) = (\sqrt{2}, \sqrt{5})$. This corresponding value represents a minimal bound for 3×3 models on a square lattice.
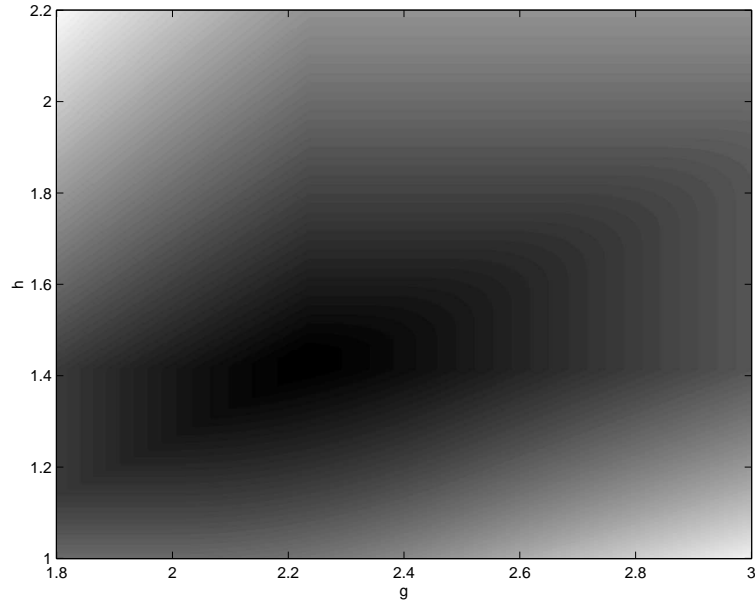
Figure 4: The criterion $ANIS_2$ in the (g, h) plane (dark (resp. light) values represent low (resp. high) values)

4   Wulff construction at zero temperature

In this section, we describe the shape one phase takes inside the other phase. We consider the shape of droplets of one phase placed in another phase as a measure of the isotropy of the models. Hereafter, we give a complete classification of the 3x3 models with this respect. We describe the droplet shape at zero temperature. We show that the droplets are polygons. The parameters (g, h) define the polygons in unique way.

Let $\Pi(g, h)$ be a shape describing the droplet given values of (g, h). To find $\Pi(g, h)$, we use the Wulff construction [7]. Let $\delta(\gamma)$ be the surface tension corresponding to the slope γ (see the definition of the surface tension in [7] or [10]). Then, the droplet is:

$$\Psi_\delta = \cap_{\underline{n} \in S^1} \left\{ x = (x_1, x_2) \in \mathbb{R}^2 : (x, \underline{n}) \leq \lambda \delta_\gamma \right\}, \tag{37}$$

where $(x, \underline{n}) = \frac{x_1}{\sqrt{1+\gamma^2}} + \frac{\gamma x_2}{\sqrt{1+\gamma^2}}$, λ defines the volume of the droplet. Instead of the surface tension δ_γ, we use the boundary tension τ_γ. The droplet $\Pi(g, h) = \Psi_\tau$. Due to the symmetries exhibited by the shapes, we can consider the part of $\Pi(g, h)$ between the lines $x_1 = 0$ and $x_2 = x_1$ on $\mathbb{R}^2$. Let $\Pi^0(g, h)$ be this part.

In the following, we describe the shapes which we call basic. For any $\gamma \in [0, 1]$ let:

$$V_\gamma = \left\{ x = (x_1, x_2) \in \mathbb{R}^2 : (x, \underline{n}) \leq \lambda \tau_\gamma \right\}.$$

Therefore, the boundary L_γ of the half-plane V_γ is given by:

$$x_1 + \gamma x_2 = \lambda \sqrt{1 + \gamma^2} \tau_\gamma. \tag{38}$$

We take $\lambda = 1$. It implies that $\Pi(g, h)$ has different volumes for different (g, h). We can consider $\Pi(g, h)$ as a set of homothetical shapes.

The following polygons $\Sigma_1, \Sigma_2, \Sigma_3$ are called the basic shapes. We only determine the parts $\Sigma_1^0, \Sigma_2^0, \Sigma_3^0$ of the polygons between the lines $x_1 = 0$ and $x_2 = x_1$ located in $\mathbb{R}_+^2$. The polygons $\Sigma_1, \Sigma_2, \Sigma_3$ are recovered using the symmetries. The polygon parts are the set:

$$
\begin{aligned}
\Sigma_1^0 &= \{(x_1, x_2) : 0 \leq x_1 \leq 1, 0 \leq x_2 \leq x_1\} \\
\Sigma_2^0 &= \{(x_1, x_2) : x_1 + x_2 \leq 1, x_1 \geq 0, x_2 \geq 0\} \\
\Sigma_3^0 &= \left\{(x_1, x_2) : 0 \leq x_1 \leq \frac{1}{\sqrt{5}}, x_1 + \frac{1}{2}x_2 \leq 1, x_1 + x_2 \leq \sqrt{\frac{2}{5}}\right\}.
\end{aligned}
\tag{39}
$$

Next propositions describe the regions where the above polygons are the droplets.

Proposition 1 *If $g \geq 3$ and $h \geq 2$ then $\Pi^0(g, h) = \Sigma_1^0$.*

Proposition 2 *If $h \leq \min\left\{1, \frac{g}{2}\right\}$ then $\Pi^0(g, h) = \Sigma_2^0$.*

Proposition 3 *If $g \leq 2$ and $h \geq \frac{2}{3}g$ then $\Pi^0(g, h) = \Sigma_3^0$.*

For the proofs of the propositions, we consider the three following points:

$$(x_1^0(\gamma), 0) \quad (x_1^1(\gamma), 1) \quad (x_1^2(\gamma), x_1^2(\gamma))$$

corresponding to the points of intersections of

$$L_\gamma = \{(x_1, x_2) : \ x_1 + \gamma x_2 = \sqrt{1 + \gamma^2}\tau_\gamma\}$$

with the lines $x_1 = 0$, $x_1 = 1$, and $x_1 = x_2$ respectively. We have

$$x_1^0 = \sqrt{1 + \gamma^2}\tau_\gamma = \begin{cases} \gamma(g - 2) + 1, & \text{if } 0 \leq \gamma \leq \frac{1}{2}, \\ \gamma(2h - g) + g - h, & \text{if } \frac{1}{2}\gamma \leq 1. \end{cases} \tag{40}$$

$$x_1^1 = \sqrt{1 + \gamma^2}\tau_\gamma - \gamma = \begin{cases} \gamma(g - 3) + 1, & \text{if } 0 \leq \gamma \leq \frac{1}{2}, \\ \gamma(2h - g - 1) + g - h, & \text{if } \frac{1}{2}\gamma \leq 1. \end{cases} \tag{41}$$

$$x_1^2 = \frac{\sqrt{1 + \gamma^2}}{1 + \gamma}\tau_\gamma = \begin{cases} \frac{\gamma}{1+\gamma}(g - 2) + \frac{1}{1+\gamma}, & \text{if } 0 \leq \gamma \leq \frac{1}{2}, \\ \frac{\gamma}{1+\gamma}(2h - g) + \frac{g-h}{1+\gamma}, & \text{if } \frac{1}{2} \leq \gamma \leq 1. \end{cases} \tag{42}$$

Proof of proposition 1. Let

$$\Delta_1 = \{(g, h) : \ \Sigma_1 \text{ is the droplet}\}$$

and

$$\Gamma_1(\gamma) = \{(g, h) : \ x_1^1(\gamma) \geq x_1^1(0)\}.$$

It is clear that:

$$\Delta_1 = \cap_{0 \leq \gamma \leq 1}\Gamma_1(\gamma).$$

It follows from eqn. (41) that $x_1^1(0) = 1$. Then for $0 \leq \gamma \leq \frac{1}{2}$, we have:

$$x_1^1(\gamma) \geq 1 \tag{43}$$

which implies $g \geq 3$ and:

$$\cap_{0 \leq \gamma \leq \frac{1}{2}}\Gamma_1(\gamma) = \{(g, h) : \ g \geq 3\}.$$

For $\frac{1}{2} \leq \gamma \leq 1$ the inequality (43) holds if $1 - g \leq 0$ and $h \geq 2$. Therefore:

$$\cap_{\frac{1}{2} \leq \gamma \leq 1} \Gamma_1(\gamma) = \{(g, h) : \ g \geq 1, h \geq 2\}.$$

$\square$

Proof of proposition 2. Let

$$\Delta_2 = \{(g, h) : \ \Sigma_2 \text{ is the droplet}\}$$

and

$$\Gamma_2(\gamma) = \{(g, h) : \ x_0^1(\gamma) \geq x_0^1(1)\}.$$

It is easy to see that:

$$\Delta_2 = \cap_{0 \leq \gamma \leq 1} \Gamma_2(\gamma).$$

Simple considerations show that:

$$\cap_{0 \leq \gamma \leq \frac{1}{2}} \Gamma_2(\gamma) = \left\{(g, h) : \ h \leq \min\left\{1, \frac{g}{2}\right\}\right\}.$$

and

$$\cap_{\frac{1}{2} \leq \gamma \leq 1} \Gamma_2(\gamma) = \left\{(g, h) : \ g \geq 1, h \geq \frac{g}{2}\right\}.$$

$\square$

Proof of proposition 3. Let

$$\Delta_3 = \{(g, h) : \ \Sigma_3 \text{ is the droplet}\}$$

and

$$\Gamma_3^1(\gamma) = \left\{(g, h) : \ x_1^0(\gamma) \geq x_1^0\left(\frac{1}{2}\right)\right\},$$

$$\Gamma_3^2(\gamma) = \left\{(g, h) : \ x_3^1(\gamma) \geq x_3^1\left(\frac{1}{2}\right)\right\}.$$

We have:

$$\Delta_3 = \cap_{0 \leq \gamma \leq \frac{1}{2}} \Gamma_3^1(\gamma) \cap \cap_{\frac{1}{2} \leq \gamma \leq 1} \Gamma_3^2(\gamma).$$
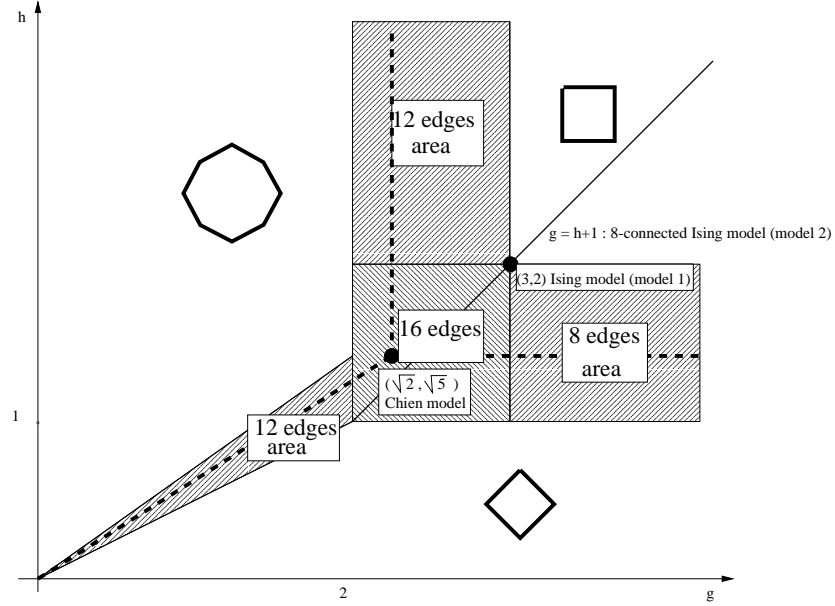
The direct calculation show that:

$$\cap_{0 \leq \gamma \leq \frac{1}{2}} \Gamma_3^1(\gamma) = \{(g, h) : \ g \leq 2\}$$

and

$$\cap_{\frac{1}{2} \leq \gamma \leq 1} \Gamma_3^2(\gamma) = \left\{(g, h) : \ h \geq \frac{3}{2}g\right\}$$

$\square$

Figure 5: The stable shapes in the (g, h) plane

On Figure 5, we show the different stable shapes in the (g, h) plane. Three main areas respectively correspond to a square, an octagon and a rhombi. These areas are separated by strips corresponding to mixture between these basic shapes with eight, twelve or sixteen edges (see hachured areas). Regular polygons are obtained on the half lines $h = \sqrt{5}, g \geq 3$, $g = \sqrt{2}, h \geq 2$ and $g = \frac{\sqrt{5}}{\sqrt{2}} h, h \leq \sqrt{2}$ (dashed lines). Finally, the more isotropic case is obtained for $(h, g) = (\sqrt{2}, \sqrt{5})$.

5   Induced effects in image processing

When segmenting an image, the data can be interpreted as an external field. To visualize the non-isotropy effect of the prior model, we first consider a 4-connected Ising model in this experiment. In this case, the boundary tension is minimized for horizontal and vertical edges. We simulate the ground state of the Ising model with a low non homogeneous external field defined by a cylinder composed of two connected parts separated by a frontier at a given angle (see Figure 6.a). The choice of a cylinder allows us to avoid boundary effects. The segmentation process shows that the model behavior depends on the angle of the frontier. The best segmentation is obtained for an horizontal frontier. For angles corresponding to a higher boundary tension, the energy minimization leads to inaccuracy in the boundary delineation. (see Figures 6.b and 6.c).

a: External field

b: Segmentation result

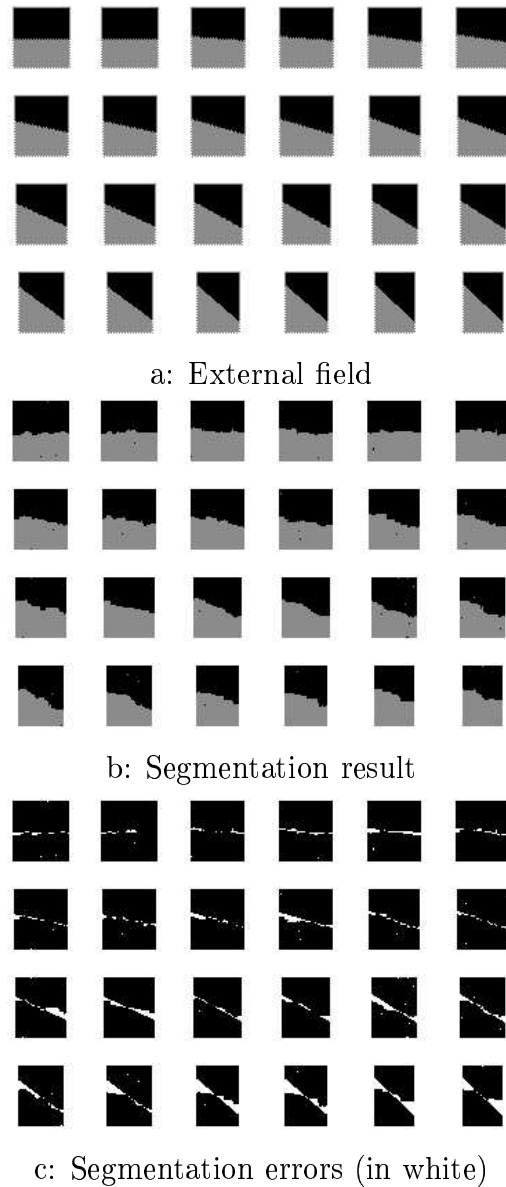c: Segmentation errors (in white)

Figure 6: Segmentation using a 4-connected Ising model as a prior: two adjacent rectangles represent the two faces of a cylinder.

We now consider a more realistic case where a binary image is corrupted by a channel noise (i.e. 20 percent of the pixels have been flipped). We want to restore the noisy image, which defines the external field in the restoration process [2, 3]. The restored image is the ground state obtained using a simulated annealing when adding a prior in a Bayesian framework. We have used three different priors: the Ising model with 4-neighbors

$(e = \frac{1}{2}, \ h = 2, \ g = 3)$, the Ising model with 8-neighbors $(e = \frac{1}{2}, \ h = \sqrt{2}, \ g = 1 + \sqrt{2})$ and the chien-model described in [9] $(e = \frac{1}{2}, \ h = \sqrt{2}, \ g = \sqrt{5})$. The obtained restorations are shown on Figure 7. We can remark that the anisotropy induced by the prior produces some deformation of the restored object. In the case of the 4-connected Ising model, we tend to obtained a square whereas the shape is closest to an octagon when using an 8-connected Ising model. The best result is obtained when using the chien-model which corresponds to the optimal point in the plane (g,h).

6 Conclusion

In this paper, we have studied some Gibbs models commonly used as prior distribution in image segmentation or restoration. The computation of the surface boundary tension and the Wulff construction at zero temperature have exhibited a non-isotropic behavior of the models. From this study, quality criteria with respect to the isotropy property have been derived to justify the choice of a particular prior model for a given image segmentation or restoration problem. Moreover, we have shown the existence of a lower bound for these criteria when considering 3×3 interaction models on a square lattice. Therefore, the size of the chosen neighborhood imposes a limit on the isotropy properties of the model. This non-isotropy induces artifacts during a segmentation or a restoration process, as shown on a synthetic example.

Future work will be devoted to the study of these model artifacts on small objects and lines in an image.

References

[1] X. Descombes, R. Morris, J. Zerubia, M. Berthod. Estimation of Markov Random Field prior parameters using Markov Chain Monte Carlo Maximum Likelihood. *IEEE Trans. on Image Processing*, 8(7):954–963, July 1999.

[2] J. Besag. Spatial interaction and statistical analysis of lattice systems. *Journal of the Royal Statistical Society, Series B*, 36:721–741, 1974.

[3] S. Geman, D. Geman. Stochastic relaxation, Gibbs distribution, and the Bayesian restoration of images. *IEEE Trans. on Pattern Analysis and Machine Intelligence*, 6(6):721–741, 1984.

[4] H.O. Georgii. *Gibbs Measures and Phase Transitions*. De Gruyter - Studies in Mathematics, 1988. Vol. 9.

a: Original image   b: Noisy image ($\tau_\gamma = 0.2$)

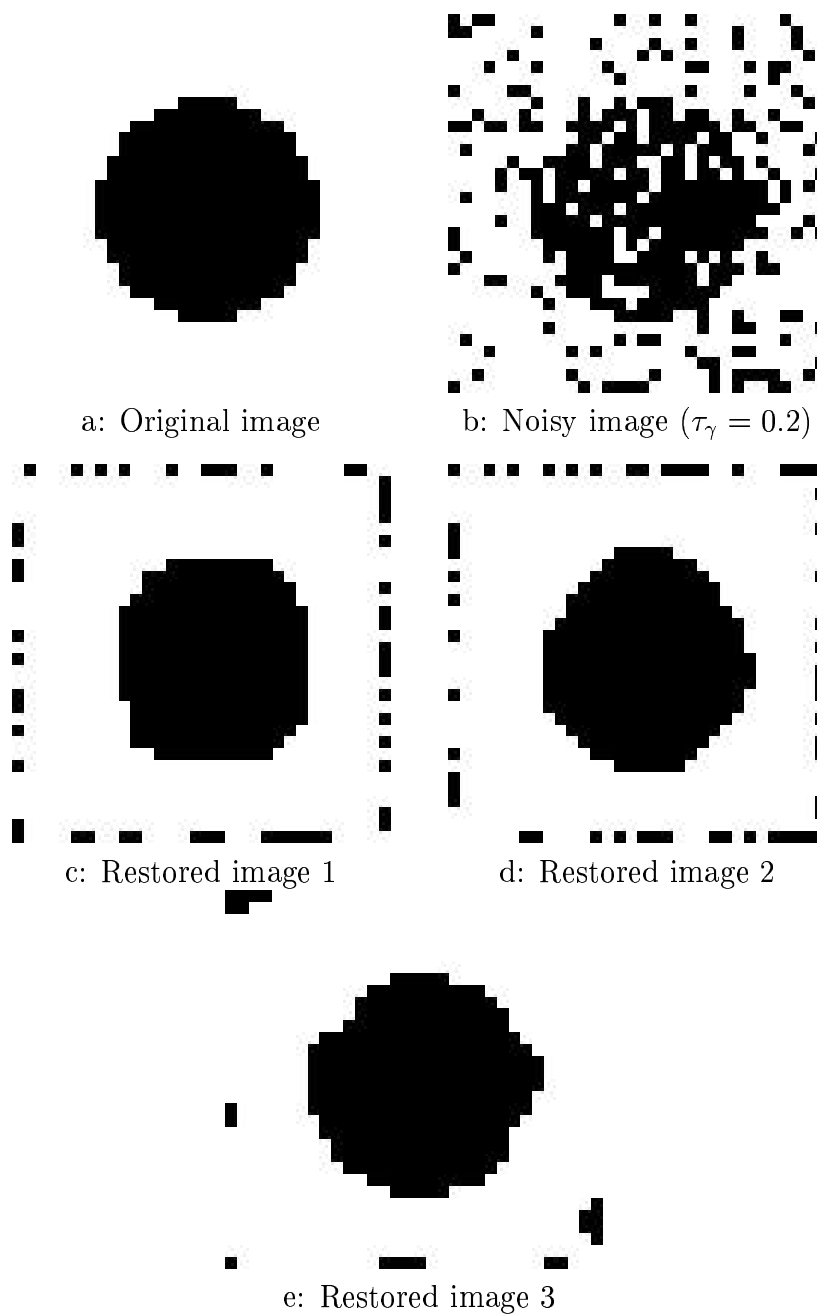c: Restored image 1   d: Restored image 2

e: Restored image 3

Figure 7: Restoration of a noisy circle (b) using the 4-connected Ising model (c), the 8-connected Ising model (d) and a chien-model (e)

[5] R. Chellappa, A. Jain. *Markov random fields : theory and application.* Academic Press, Inc. Collective work, 1993.

[6] R. Morris. Auxilliary variables for Markov Random Fields with higher order interactions. *submitted to Statistics and Computing Journal*, 1999.

[7] R. Dobrushin, R. Kotecky, S. Shlosman. Wulff construction: a global shape from local interaction. *Amer. Math. Soc. Ed.*, page 235, 1992.

[8] A. Maruani, E. Pechersky, M. Sigelle. On Gibbs fields in image processing. *Markov Processes and Related Fields*, 1:419–442, 1995.

[9] X. Descombes, J.F. Mangin, E. Pechersky, M. Sigelle. Fine structures preserving model for image processing. In *Proc. 9th SCIA, Uppsala, Sweden*, pages 349–356, 1995.

[10] T. Bodineau, D. Ioffe, Y. Velenik. Rigorous probabilistic analysis of equilibrium crystal shapes, preprint, 1999.